Precise International Roughness Index Calculation

Filip Šroubek*, Michal Šorel*, Josef Žák**

*The Czech Academy of Sciences, Institute of Information Theory and Automation, Pod Vodarenskou vezi 8, Prague, Czech Republic. Email: sroubekf@utia.cas.cz

**CTU in Prague, Faculty of Civil Engineering, Department of Construction Management and Economics, Thakurova 7, Prague, Czech Republic. Corresponding author, e-mail: josef.zak@fsv.cvut.cz

Abstract

Roadway infrastructure management focuses on quality of the road surfaces which influences the pavement longevity and riding quality. The road surface quality can be expressed in many ways from which the International Roughness Index has been recognized widely around the developed countries. This paper summarizes the derivation of International Roughness calculation and proposes a new numerical method for its computation. Compared to original Sayers's method, it does not use iterative approximation, which makes it much faster for non-uniformly sampled road data. This is useful, for example, for profiles generated from LIDAR point clouds. The method can be used for arbitrary polynomial model of segments between elevation samples. Except the Fortran code listed in the original paper, the code for the original algorithm has not been publicly available and most researchers relied on the ProVAL software with several limitations, including uniform sampling, the lack of automation, and little control over the influence of resampling methods and the initialization of the quarter-car simulation procedure. We provide Matlab codes for both the original method and the algorithm newly proposed in this paper.

Keywords

Asphalt layer roughness; international roughness index; LIDAR; point cloud

Acknowledgement

Data availability

All data and Matlab code of the proposed method are available in an online repository https://github.com/michalsorel/iri.

1   Introduction

An important criterion used for pavement monitoring is surface smoothness. The smoothness is tracked by the road maintenance agency and perceived by the road users. It was proved in (Sayers et al., 1986b) that highway users judge the condition of a highway by the riding experience when they travel over the highway. The pavement surface smoothness is related to road users' riding comfort and, most importantly, to road safety (Kirbas 2018).   Is is also one of the determinants of road user cost, as indicated in (Sayers et al. 1986b). The choice of a proper pavement reconstruction design and technology has always been a task combining engineer's knowledge and experience. Many aspects that embeds empirical approach in pavement design persist in the asphalt pavement industry till today (Monismith 2012). The engineer's goal is to effectively design and construct a desired pavement layer while meeting all standardized requirements, design criteria and contracting agencies' demands. However, many disorders during the construction work, such as flawed mix design and errors in the laydown process, result in an immediate decrease of the constructed layer quality. Some of these disorders are present right after the layer construction, and some of them take their effect when traffic loading and weather conditions occur during the pavement's lifetime. Thus in terms of pavement reconstruction, the engineer's challenge is even more profound when taken into account pavement deterioration caused by climatic conditions, traffic loading, subgrade deterioration (Rys and Jasukula 2018).

Based on data collected over ten years from more than 400 test sections, (Janoff 1996) suggested that the initial smoothness is related to the pavement long-term roughness and durability in regard of the pavement cracking and overall deterioration. These findings are today proved by the mechanical analysis addressing the effect of flexible pavement viscoelasticity in relation to dynamic loading increased with the pavement surface roughness (Chabot et al. 2010; Chen et al. 2011; Zak et al. 2015; Xu et al. 2014; Zak 2016).

The asphalt layer roughness has been used in many project specifications over the US and European countries to set pay adjustments based on the desired threshold. Nowadays, even in Public-Private-Partnership schemes and advanced design-build projects, roughness is one of the specifically set quality criteria. Furthermore, advanced design techniques and the use of construction machine control systems help to achieve these contract requirements (Prikryl et al. 2011).

The need to measure the pavement surface smoothness led to the development of various devices. Very simple and still in use are the rod and level, profilographs, where the Californian profilograph may be mentioned as one of the early developed devices (Scofield et al. 1992), and response type devices also known as Reponse Type Road Roughness Measuring systems. With the advances in technology, several automated devices were developed to measure the pavement smoothness (Choubane et al. 2002; Monismith 2012) including smartphones and other inexpensive sensors (Khalifeh et al. 2018; Chatterjee and Tsai 2020; Alatoom and Obaidat 2021).

The use of various roughness measuring devices led to the development of many roughness indices, such as
  Profilograph Index (PrI),   Mean Roughness Index (MRI),   Quarter-car Index,   root-mean-square vertical acceleration and   rod and level surface smoothness measurement (roughness), whose review may be found in (Mucka 2016; Boscaino and Pratico 2001; Chemistruck et al. 2009; Sayers and Karamihas 1998; Wilde 2007; Willet et al. 2000).

With many roughness measuring devices and indices that were difficult to correlate between them, the World Bank conducted the International Road Roughness Experiment (IRRE) in Brazil in 1982, with the aim of harmonizing the different indices (Sayers et al. 1986a). When analyzing the data, it was shown that nearly all the roughness measuring devices in use around the world produce measures on the same scale, if the scale was suitably selected, and the development of the International Roughness Index (IRI) was initiated. Due to its stability over time and transferability all over the world, IRI has become the most widely employed pavement index, with examples in developed countries (Zeiada et al. 2019, Pérez-Acebo et al. 2021, Mohammadi et al. 2019) and in developing countries (Nguyen et al. 2019; Pérez-Acebo et al. 2019, Obungunta and Matsushima 2020).

Light detection and ranging (LiDAR) and photogrammetry are the advanced geoinformation technologies that are able to capture the highway surface geolocation in large scale. Both LiDAR and photogrammetry are methods that generate point clouds with billions of points. These big data can be utilized to address the IRI, yet the data are often not sampled on regular grids.

2   Contributions

In this paper, we propose a novel method to compute IRI from elevation measurements taken at arbitrary regular intervals and possibly also any irregular intervals. We provide implementation of the method in the Matlab programming language.

Our work was motivated by the need to implement the computation of IRI as a software package component developed in our research institute. The software package utilizes the point cloud data captured by LiDAR. The code for the original algorithm in a computer language suitable for our purposes (Matlab or Python) was not publicly available and the only free option was ProVAL software (ProVAL), which has several limitations. ProVAL has only a graphical user interface, which means that repeated IRI computation cannot be automated. ProVAL works only with uniform sampling of elevation profiles. In the non-uniform case, the user must first resample data on a uniform grid, which inevitably influences the value of IRI subsequently computed. Finally, the code of the software is not available, which complicates more elaborate analysis of smoothness. For example, if we want to analyze the influence of the quarter car model initialization in the IRI computation.

The IRI computation, as described in the World bank proposal (Sayers et al. 1986b), and later in (Sayers 1995), solves an inhomogeneous linear ordinary differential equation modeling the motion between sprung and unsprung masses of a car moving by a constant speed along a measured section of the road.

In the original approach, the equation is solved by the state transition method. As an alternative, we propose a solution based on the method of variation of constants (Teschl 2012). This approach gives the same results but offers greater flexibility and speed, especially for non-uniform sampling of input road profile. Ability to use non-uniform sampling can be useful in several situations. For example, elevation profile generated by intersection of a wheel path with edges of a triangulated point cloud has irregularly spaced samples. Another situation is a measurement with imprecise odometer, which systematically over or underestimates distance, and we want to rectify the results.

While non-uniform sampling is in theory possible even in the original method, the iterative

computation of the exponential of the transition matrix makes the computation impractical, which also explains why this option is not available in ProVAL. Similarly to the original solution, IRI can be computed efficiently by the proposed method both for overlapping (floating-window mode) and non-overlapping road sections. Finally, in contrast to the original algorithm, which requires linear segments between road samples, the proposed method can incorporate any polynomial model without increasing computational requirements. While this is partially a theoretical advantage, because IRI assumes piece-wise linearity by definition, this could be useful in the research of IRI alternatives.

    To summarize, the proposed solution works with equal efficiency for
        • uniform and non-uniform sampling of the road profile,
        • overlapping and non-overlapping road sections,
        • any polynomial model of road segments between samples.
    We also provide the code of the proposed method in Matlab, which is suitable for computing IRI automatically on large set of road profiles.

3   International Roughness Index

This section contains a concise summary of the IRI definition based mainly on (Sayers et al. 1986b; Sayers 1995).

    IRI is computed from a single longitudinal profile, represented by a sequence of elevation measurements. The sample interval should be no larger than 300 mm for accurate measurements. According to (Sayers 1995), a vertical resolution of 0.5 mm is suitable for all situations. The slope of the road between samples is assumed to be constant.

    The computation consists of three steps.
        1.   the profile is smoothed by a box filter of length 250 mm
        2.   the ride of an ideal car (Golden Car) is simulated using the quarter-car model at a speed of 80 km/h.
        3.   IRI of a road section is defined as an accumulated suspension motion divided by the length of the section.

    The quarter-car model using Newton's laws of motion is described by four first-order differential equations, which can be written in matrix form as

$$\frac{dx}{dt} = x' = Ax(t) + bh(t) \tag{1}$$

with an initial condition $x(0) = x_0$. Quantities x, A and b are defined as follows:

$$x(t) = [z_s(t), z_{s'}(t), z_u(t), z_{u'}(t)]^T, \tag{2}$$

$$A = \begin{bmatrix} 0 & 1 & 0 & 0 \\ -k_2 & -c & k_2 & c \\ 0 & 0 & 0 & 1 \\ k_2/u & c/u & -(k_1 + k_2)/u & -c/u \end{bmatrix}, \tag{3}$$

$$b = [0,0,0, k_1/u]^T, \tag{4}$$

where $z_s(t)$, $z_u(t)$ and $h(t)$ are height of sprung mass, height of unsprung mass and profile elevation, respectively. The parameters for the *Golden Car* model are defined as $c = 6.0 \text{ s}^{-1}$,

$k_1 = 653 \text{ s}^{-2}$, $k_2 = 63.3 \text{ s}^{-2}$ and $u = 0.15$. Time derivatives are indicated with a prime mark. Time is related to a longitudinal distance by the simulated speed of vehicle, as shown in Equation (5):

$$t = x/V ,\qquad(5)$$

where x is longitudinal distance and V is the simulated forward speed defined as 80 km/h for the IRI. Vector $x(t)$ contains four state variables (height and speed of sprung and unsprung mass) that completely describe the simulated system in time.

The IRI of a section of length L is defined as in Equation (6):

$$IRI = \frac{1}{L}\int_0^{L/V} |z_{s\prime}(t) - z_{u\prime}(t)|dt ,\qquad(6)$$

which is as an accumulation of the absolute suspension motion (distance of sprung and unsprung masses) divided by L. A common approach is to divide the road profile into segments of constant length (common length's are $L = 20$ m or $L = 100$ m) and the IRI is calculated in each segment separately. An alternative is computation in each profile sample by a moving window of length L.

IRI is linear in two senses. First, the definition in Equation (6) implies that the average IRI of two segments of the same length equals the IRI of the segments taken together. Second, multiplication of the elevation input data by a scalar constant results in the multiplication of IRI by the same value. This comes from the linearity of both Equations (1) and (6).

4   Proposed solution

The proposed solution is based on the method of variation of constants; see (Teschl 2012) Chapter 3.4. Using this method, the IRI problem presented in Equation (1) has an analytical solution $x(t)$, which is the sum of a general solution $x_h(t)$ of the associated homogeneous system $x'(t) = Ax(t)$ and a particular solution $x_p(t)$ of the nonhomogeneous system: $x(t) = x_h(t) + x_p(t)$. Let $M(t)$ be a fundamental (also called principal) matrix with columns that correspond to the solution of the homogeneous system, i.e. $M'(t) = AM(t)$. The fundamental matrix is constructed from eigenvalues and eigenvectors of A; see e.g. (Lay et al. 2016) Chapter 5.7. The constant form of A guarantees that $M(t)$ is invertible for every t. The solution of the associated homogeneous system that satisfies the initial condition is $x_h(t) = M(t)M(0)^{-1}x_0$. The general solution of Equation (1) is then given by Equation (7):

$$x(t) = M(t)M(0)^{-1}x_0 + M(t)\int_0^t M(s)^{-1}bh(s)ds .\qquad(7)$$

The integral in the second term can be calculated analytically for certain forms of $h(t)$ and this allows us to express the general solution explicitly. An example of the form that allows explicit solution are piece-wise polynomials. In practice, the road profile is sampled and h is a discrete variable represented as a sequence $\{h_i\}_{i=0}^N$, where h_i is the profile elevation at distance x_i and time $t_i = x_i/V$. We assume that $\{x_i\}$ is an increasing sequence with $x_0 = 0$ and $x_N = L$. Note that the sampling need not be uniform. Let $p(t|c_i)$ denote a polynomial function defined by a set of coefficients c_i. The function is set to zero everywhere except on the interval $\langle t_{i-1}, t_i \rangle$. The number of coefficients in c_i depends on the polynomial degree and the coefficient values are calculate from $\{h_i\}$ and $\{t_i\}$ according to the used interpolation method. The polynomial interpolation of $\{h_i\}$ is expressed as $h(t) = \sum_i p(t|c_i)$ and then the integral can be calculated

analytically on every interval $\langle t_{i-1}, t_i \rangle$ by Equation (8):

$$F(t_{i-1}, t_i, c_i) \equiv \int_{t_{i-1}}^{t_i} M(s)^{-1} bp(s|c_i) ds. \tag{8}$$

We used Matlab Symbolic Math Toolbox to find the analytical expression for F.

The general solution of Equation (1) at time t for a polynomial interpolation of the profile sequence $\{h_i\}$ and the corresponding time samples $\{t_i\}$ is given by Equation (9):

$$x(t) = M(t)(M(0)^{-1} x_0 + \sum_{k=1}^{K} F(t_{k-1}, t_k, c_k) + F(t_K, t, c_{K+1})), \tag{9}$$

where the index K is such that $t_K < t \leq t_{K+1}$.

We are often interested only in the discrete solution $x_i \equiv x(t_i)$ at time samples $\{t_i\}_{i=1}^{N}$, which is the special case of Equation (9),

$$x_i = M(t_i)\big(M(0)^{-1} x_0 + \sum_{k=1}^{i} F(t_{k-1}, t_k, c_k)\big). \tag{10}$$

The IRI is then approximated by a discrete form of Equation (6), i.e.

$$IRI \approx \frac{1}{L} \sum_{i=1}^{N} |x_i(2) - x_i(4)|(t_i - t_{i-1}), \tag{11}$$

where $x_i(2)$ and $x_i(4)$ are the second, $z_{s'}$, and the forth, $z_{u'}$, element of the vector $x(t_i)$, respectively.

Since IRI (Sayers 1995), is a sum of contributions from individual time intervals, the dense computation by the moving window can be computed very efficiently – IRI in the next road section is nothing else than just the IRI value from the previous section plus the contribution of the new time interval $t_{N+1} - t_N$, minus the contribution of the interval $t_2 - t_1$.

The final aspect of the IRI definition we should mention is the initialization of the simulation. In (Sayers 1995), the initial state of simulation is recommended to be set using the average slope over the first $L_0 = 11$ m. In our case, this corresponds to the time $T_0 = L_0/V$ to travel the distance L_0, which implies

$$x_0 = [h(0), (h(T_0) - h(0))/T_0, h(0), (h(T_0) - h(0))/T_0]. \tag{12}$$

Nevertheless, at 80 km/h even the best initialization influences simulation for about 20 m, which means that ideally the simulation should be started at least 20 m before the start of the measurement. In addition, even if IRI is computed on non-overlapping profile segments, the simulation should be run for entire profile without re-initialization for each segment. This is a natural behavior of a real vehicle going without any interruptions.

5   Experiments

To check correctness of the proposed algorithm, we implemented also the original Sayers's methods and verified that both give exactly (to the machine precision) the same results. Next, we compared the IRI values computed by the proposed algorithm and ProVAL application on a number of elevation profiles. As an example, we show this comparison for a profile of a damaged road acquired by a mobile LIDAR system.

In Figures 1 and 2, we compare IRI in sections of 100 m and 20 m, respectively. We can see that the values provided by ProVAL are close to those from our algorithm (0.4 % and 1.5 % relative error). Similarly, in Figure 3, we show the same comparison for segments of length 1 m.

Since IRI is in this case averaged on much smaller segments, their values tend to differ more than for longer IRI segments. Interestingly, ProVAL seems to systematically "undershoot" peak values of IRI. The next experiment demonstrates the ability of the proposed algorithm to work with arbitrary sampling including irregularly sampled data. We show that resampling necessary in the standard method (Sayers 1995) smooths the elevation profile and consequently lowers the value of IRI. For this purpose, we randomly generated 200 continuous elevation profiles with $IRI = 1$ according to the Gaussian one-parametric model with fixed waviness $w = 2$ as described in the ISO standard 8608 (ISO8608 1995; Bogsjö et al. 2012). These profiles have the same power spectrum but each profile and each frequency has different random phase. An example of such profile is shown in Figure 4. To completely eliminate the influence of the initialization, we constructed the profiles to be periodic with period 100 m and measured IRI on the last 100 m.
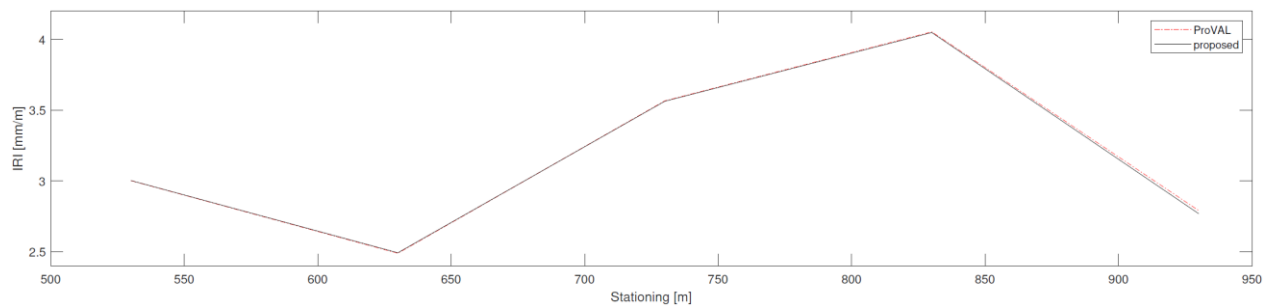
Figure 1: Comparison of IRI values computed by ProVAL and the proposed algorithm for non-overlapping segments of length 100 m. Elevation data were sampled with 0.25 m interval from a triangulation of a LIDAR point cloud. Elevation data were sampled every 0.25 m.
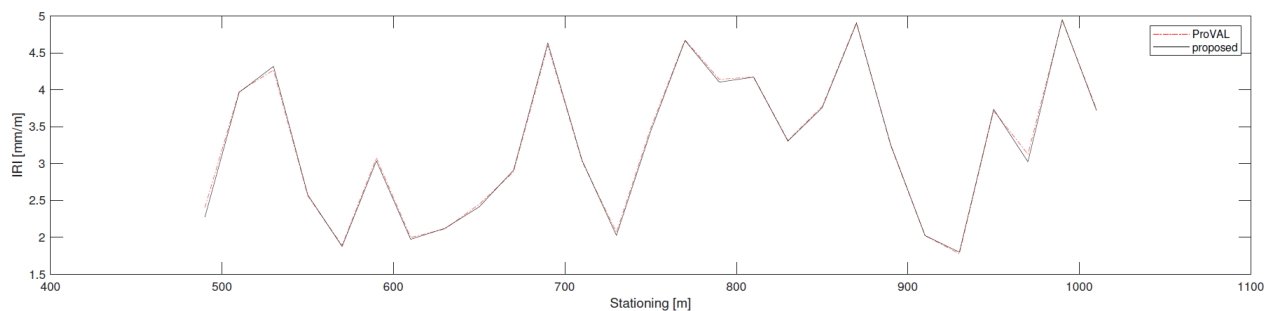
Figure 2: Comparison of IRI values computed by ProVAL and the proposed algorithm for non-overlapping segments of length 20 m.
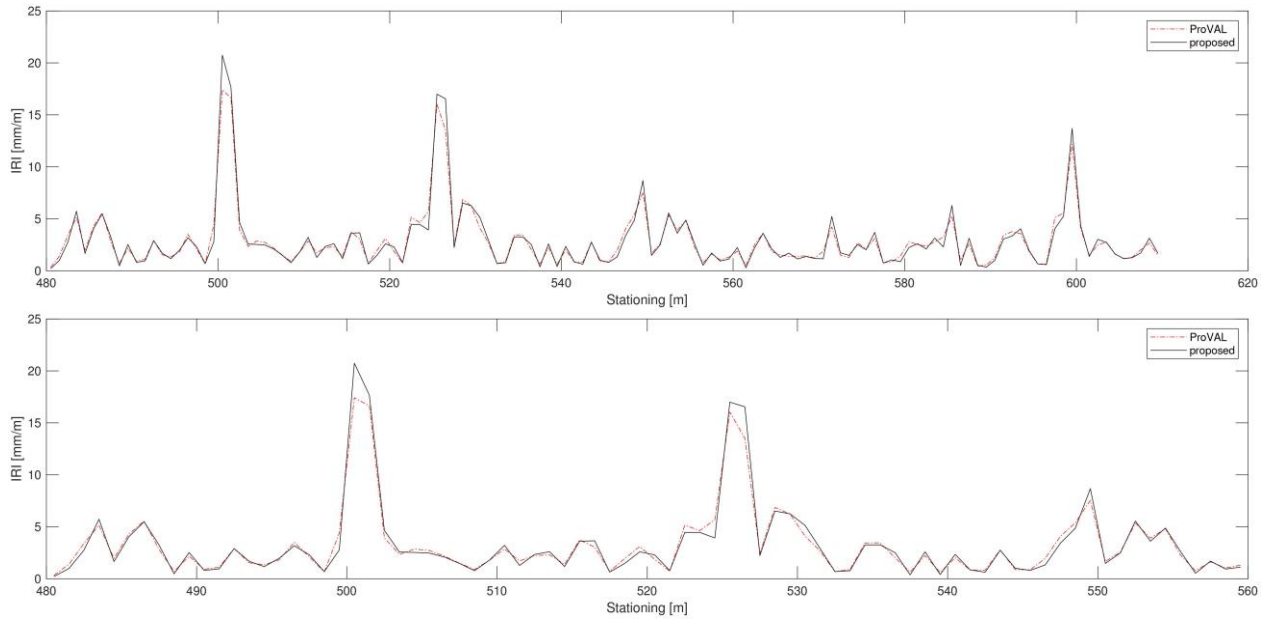
Figure 3: Comparison of IRI values computed by ProVAL and the proposed algorithm for non-overlapping segments of length 1 m. Both graphs show the same data on different scales.
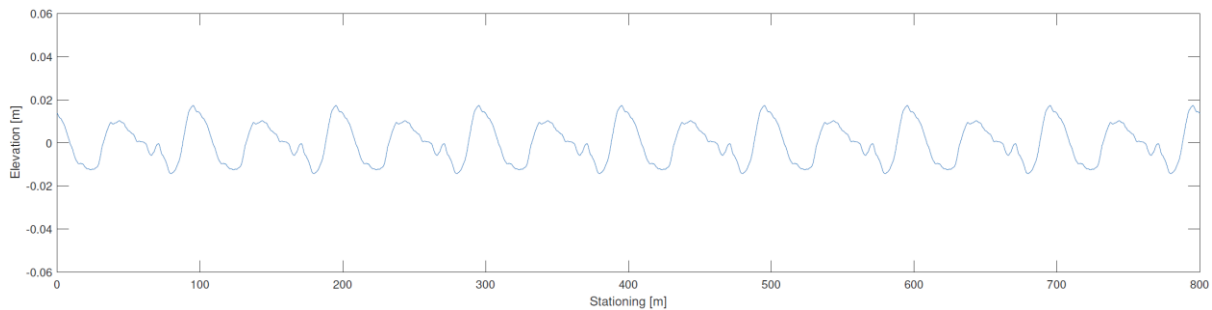
Figure 4: An artificial road with IRI $= 1$. This is an example of one road generated in the experiment demonstrating the influence of resampling. These roads are intentionally made periodic to completely eliminate the influence of initialization.

Let us assume that we need to compute IRI on a 100 m interval with a sampling step 0.25 m but the samples are mistakenly taken shifted by 0.125 m, i.e. half of the sampling interval. Assume that this shift is known. Whereas the standard method (Sayers 1995) first requires resampling to correct positions, the proposed method computes IRI directly for arbitrary coordinates. Results are shown in Table 1, where they are compared with the IRI of the continuous profile. The table summarizes the mean value of IRI, the root means square error of IRI estimation and the maximum error over the set of 200 profiles. Table 2 shows the results of an analogous experiment but for a larger sampling step of 0.5 m. Note that in these experiments the numbers for the correct sampling and the proposed method are mostly same to three decimal places but may differ in the fourth decimal place not shown in the tables.

Method	mean IRI	RMSE	Max. error
Continuous profile	1	0	0
Correct sampling	0.994	0.006	0.008
Resampling	0.986	0.014	**0.019**
Proposed direct method	0.994	0.006	**0.009**

Table 1: Resampling errors for sampling step 0.25 m.

Method	mean IRI	RMSE	Max. error
Continuous profile	1	0	0
Correct sampling	0.980	0.020	0.029
Resampling	0.956	0.045	**0.061**
Proposed direct method	0.980	0.020	**0.029**

Table 2: Resampling errors for sampling step 0.5 m.

We see that resampling causes lower IRI by smoothing the elevation profile. Even for step 0.25 m, i.e. less than the recommended 0.3 m (Sayers 1995), the error can achieve almost 2 % of the IRI value with the average error about 1.4 %. For a slightly longer step of 0.5 m, the maximum error rises to 6 % and the average error to 4.5 %. A rule of thumb in these experiments is that resampling approximately doubles the error caused by discrete sampling of the profile. For more dense sampling, the error becomes negligible, yet it should be taken into account for sampling steps around the recommended value of 0.3 m.

The code of the proposed method is provided in Matlab at GitHub, Python implementation is planned in near future (https://github.com/michalsorel/iri). We verified that for segments of length 20 m and 100 m, the code gives results very close to those computed by ProVAL and can be used as its alternative for all practical purposes.

6   Conclusion

The asphalt layer roughness is being used in many projects specifications over the US and European countries to asses quality of pavements. The newly proposed computation method allows superior utilization of three-dimensional (3D) big data such as light detection and ranging (LiDAR) point clouds to compute IRI.

Moreover LiDAR technologies allow the data aquisition and by utilization of proposed method IRI computation even in urban areas where the conventional measurement techniques can not be utilized.

The proposed method works with arbitrary even non-uniform sampling of elevation profiles, which avoids resampling that otherwise causes underestimation of the IRI value. For non-uniform sampling of road profile, the method is significantly more efficient than the original method (Sayers and Karamihas 1998).

References

K. Bogsjö, K. Podgórski, and I. Rychlik. Models for road surface roughness. *Vehicle System Dynamics*, 50(5):725–747, 2012.

G. Boscaino and F. Pratico. A classification of surface texture indices of pavement surfaces. *Bulletin Des Laboratoires Des Ponts et Chaussees*, 234:17–34, 2001.

A. Chabot, O. Chupin, L. Deloffre, and D. Duhamel. Viscoroute 2.0 a tool for the simulation of moving load effects on asphalt pavement. *Road Materials and Pavement Design*, 11:227–250, 06 2010.

A. Chatterjee and Y. Tsai. Training and testing of smartphone-based pavement condition estimation models using 3d pavement data. *Journal of Computing in Civil Engineering*, 34(6):04020043, 2020.

Y. I. Alatoom and T.I. Obaidat. Measurement of Street Pavement Roughness in Urban Areas Using Smartphone. *International Journal of Pavement Research and Technology, 2021.*

H.M. Chemistruck, Z.R. Detweiler, J.B. Ferris, A.A. Reid, and D.J. Gorsich. Review of current developments in terrain characterization and modeling. In Dawn A. Trevisani, editor, *Modeling and Simulation for Military Operations IV*, volume 7348, pages 190 – 201. International Society for Optics and Photonics, SPIE, 2009.

Ewan Y.G. Chen, Ernian Pan, Timothy S. Norfolk, and Qiang Wang. Surface loading of a multilayered viscoelastic pavement. *Road Materials and Pavement Design*, 12(4):849–874, 2011.

Bouzid Choubane, Ronald McNamara, and Gale Page. Evaluation of high-speed profilers for measurement of asphalt pavement smoothness in florida. *Transportation Research Record*, 1813:62–67, 01 2002.

J. Howe, Jeffrey Chrstos, Richard Allen, Thomas Myers, Dongchan Lee, Chi-Ying Liang, David Gorsich, and Alexander Reid. Quarter car model stress analysis for terrain/road profile ratings. *International Journal of Vehicle Design*, 36, 01 2004.

ISO8608. *ISO 8608 : Mechanical Vibration, Road Surface Profiles, Reporting of Measured Data: International Standard*. International Organization for Standardization, ISO, 1995.

M.S. Janoff. *Pavement smoothness*. Information Series 53. National Asphalt Pavement Association, 1996.

V. Khalifeh, A. Golroo, and K. Ovaici. Application of an inexpensive sensor in calculating the international roughness index. *Journal of Computing in Civil Engineering*, 32(4):04018022, 2018.

Kirbas. IRI Sensitivity to the Influence of Surface Distress on Flexible Pavements. *Coatings*, 8, 271, 2018.

D.C. Lay, S.R. Lay, and J.J. McDonald. *Linear Algebra and Its Applications (5th Edition)*. Pearson, 2016.

A. Mohammadi, L.A. Jimenez, and F. Elsaid. Simplified pavement performance modeling with only two-time series observations: A case study of Montreal Island. *Journal of*

Transportation Engineering, Part B: Pavements, 145(4), 2019

Carl L. Monismith. Flexible pavement analysis and design-a half-century of achievement. In *Geotechnical Engineering State of the Art and Practice*, pages 187–220, 2012.

Peter Mucka. International roughness index specifications around the world. *Road Materials and Pavement Design*, pages 929–965, 06 2016.

H.L. Nguyen et al. Adaptive Network Based Fuzzy Inference System with Meta-Heuristic Optimizations for International Roughness Index Prediction. *Applied Science*, 9, 4715, 2019.

F. Obunguta, and K. Matsushima. Optimal pavement management strategy development with a stochastic model and its practical application to Ugandan national roads. *International Journal of Pavement Engineering*, doi: 10.1080/10298436.2020.1857759, 2020.

H. Pérez-Acebo, N. Mindra, A. Railean, and E. Rojí. Rigid pavement performance models by means of Markov Chains with half-year step time. *International Journal of Pavement Engineering*, 20, 830-843, 2019.

H. Pérez-Acebo, H. Gonzalo-Orden, D.J.Findley, and E. Rojí. Modeling the international roughness index performance on semi-rigid pavements in single carriageways. *Construction and Building Materials*, 272, 121665, 2021.

M. Prikryl, L. Kutil, and J. Zak. 3d laser scanning measurement technology, sweden road 41 (väg 41) bergham-gullberg. In *Asphalt Pavements*, pages 23–32, Prague, 2011. Pragoprojekt.

ProVAL. Profiler viewing and analysis software (version 3.6.).

D. Rys and P. Jaskula. Effect of overloaded vehicles on whole life cycle cost of flexible pavements. In *Testing and Characterization of Asphalt Materials and Pavement Structures*, pages 104–117. Springer, 07 2018.

M.W. Sayers, T. D. Gillespie, and C. Quieroz. International Road Roughness Experiment Establishing Correlation and a Calibration Standard for Measurements. Technical Paper WTP45, The World Bank, Washington, D.C., USA, 1986a.

M.W. Sayers, T.D. Gillespie, and W.D.O. Paterson. Guidelines for conducting and calibrating road roughness measurements. Technical Report WTP46, The World Bank, Washington, D.C., USA, 1986b.

M. W. Sayers and S.M. Karamihas. *The Little Book of Profiling*. University of Michigan, MI, USA., 1998.

M. W. Sayers. On the calculation of international roughness index from longitudinal road profile. *Transportation Research Record*, 1501:1–12, 1995.

L. Scofield, S. Kalavela, and M. Anderson. Evaluation of california profilograph. *Transportation Research Record*, 1348:1–7, 1992.

G. Teschl. *Ordinary Differential Equations and Dynamical Systems*. Graduate studies in mathematics. American Mathematical Soc., 2012.

W. James Wilde. Implementation of an international roughness index for mn/dot pavement construction and rehabilitation. Technical Report MN/RC-2007-09, Minnesota State University, Minnesota Department of Transportation, St. Paul, USA, 2007.

M. Willet, G. Magnusson, and B.W. Ferne. Filter experiment – theoretical study of indices. *FEHRL Tech. Note 2000/02*, 2000.

H.L. Xu, Y. Yuan, T.J. Qu, and J.R. Tang. Dynamic model for a vehicle-pavement coupled system considering pavement roughness. *Journal of Vibration and Shock*, 33(19):152–156, 2014.

J. Zak, Carl L. Monismith, and D. Jaruskova. Consideration of fatigue resistance tests

variability in pavement design methodology. *International Journal of Pavement Engineering*, 16(1):91–96, 2015.

J. Zak. On laser scanning, pavement surface roughness and international roughness index in highway construction. In *E&E Congress*, Prague, Czech Republic, 1-9, 2016.

Zeiada et al. Investigation and modeling of asphalt pavement performance in cold regions. *International Journal of Pavement Engineering*, 20(8), 986-997, 2019.